Tuning Electronic and Ionic Conductivities in Composite Materials for Electrochemical Devices

Nerea Casado,[*,†] *Sara Zendegi,*[†] *Rafael del Olmo,*[†] *Antonio Dominguez-Alfaro,*[†,§] *Maria Forsyth*[*,†,‡,⊥]

[†]POLYMAT, University of the Basque Country UPV/EHU, Joxe Mari Korta Center, Ave. Tolosa 72, 20018 Donostia-San Sebastián, Spain.

E-mail: Nerea.casado@ehu.eus, maria.forsyth@deakin.edu.au

[‡]ARC Centre of Excellence for Electromaterials Science (ACES), Deakin University, Burwood, VIC 3125, Australia

[⊥]Ikerbasque, Basque Foundation for Science, E-48011 Bilbao, Spain

[§]Present address: CIC biomaGUNE, Carbon BioNanotechnology group, Miramon Pasealekua, 182, San Sebastian 20014, Spain.

ABSTRACT. Mixed conductors having both high ionic and electronic conductivity are needed in membrane electrode assemblies (MEA) present in electrochemical devices from fuel cells, to supercapacitors and all battery chemistries. Typically, carbon black, binders and redox active materials are combined to make an electrode assembly into which a liquid electrolyte can

impregnate. Solid state devices require the ionic conduction built into the MEA. In this case, a material which can provide both electronic and ionic conduction as well as a redox functionality is described based on PEDOT-Cl as both the electronic conductor and the redox active component whilst an organic ionic plastic crystal [C_2mpyr][FSI] is present as both binder and ionic conductor. Surprisingly, both the electronic and ionic conductivity of the composite are enhanced relative to the pure components by a factor of ×9 for electronic and ×180 for ionic. The mixed conducting composites are demonstrated to retain their redox activity in aqueous electrolytes, and, in the optimum case, 103 F g^{-1} and 296 mF cm^{-2} capacitance values are obtained for low and high mass loading electrodes. These materials demonstrate an innovative approach to prepare electrode assemblies where all three functionalities are incorporated into the materials. ie. electronic, ionic and redox activity for future energy devices.

KEYWORDS: Organic mixed ionic/electronic conductors, conducting polymers, organic ionic plastic crystal, PEDOT, electroactive materials

1. INTRODUCTION

Mixed ionic and electronic conduction plays a key role in energy storage systems (ESS) such as fuel cells, batteries and supercapacitors.[1] The operating mechanism of these devices involves the concomitant processes of ion conduction along with the electron transfer and this determines the efficiency of the device. For instance, electrodes for rechargeable lithium-ion batteries are typically built with an active material ($LiCoO_2$, $LiFePO_4$), and other indispensable additives such as a binder (polyvinylidene difluoride, PVdF) and an electron conducting material (carbon particles).[2] Mixed ionic-electronic conductors (MIECs) are potentially ideal additives which offer

not only the electron conduction but at the same time ionic conductivity that makes possible the transport of the ions through the electrode. This could have a major influence on electrode kinetics in an all solid-state device.

The origin of MIECs comes from inorganic systems widely studied and previously applied in membranes[3] and fuel cells,[4] showing outstanding ionic conductivity and thermal stability. Nevertheless, the properties of π-conjugated conducting polymers, which are intrinsic MIECs,[5] such as semi-metallic electronic conductivity, reversible electrochemical activity and ease to manufacture, makes them highly promising materials that could act as binder as well.[6]

Although the understanding of the mechanism and electronic-ionic coupling is not clear yet, conducting polymers have been successfully employed in a large range of applications (such as chemical sensors,[7] ion pumps,[8] transistors,[9] electrochromic displays[10] and energy storage systems.[11] They have been used in energy-storage devices as a link between batteries and capacitors, giving more energy than pure capacitors but also being able to cycle faster than batteries.[12] From the large variety of conducting polymer derivatives, typically based on polyaniline, polypyrrole and polythiophene, poly(3,4-ethylenedioxythiphene):polystyrene (PEDOT:PSS) has sparked much interest because of its flexibility, stability and easy processing. The electronic conductivity of the conjugated conducting polymers is given by the movement of holes and electrons through charge defects, namely polarons and bipolarons, as result of a p-doping mechanism. These positive charges are stabilized by counter anions (ie. PSS) often called dopants. The commercially available PEDOT:PSS (Clevios PH1000) is typically in an optimum weight ratio of 2.5:1 with a relatively poor electronic conductivity of 0.2 S cm^{-1} at room temperature.[13] Although PSS makes the solution processing possible, at the same time it limits the electronic

conductivity.[14] Many studies have been published based on the enhancement of mechanical properties,[15] electronic conductivity [16,17] or hybrid architectures.[18]

As a result of the poor electronic conductivity of PEDOT:PSS, other systems have appeared with different counter anions including tosylate,[19] bromide[20] or chloride[12] with higher electronic conductivities. At the same time, different strategies to increase the electronic conductivity have shown excellent results by post treatment with either alcohols,[16] high boiling point solvents[17] or acids,[21] adding ionic liquids[22] and creating nanolayers.[23] Ionic liquids based on imidazolium cation showed an improvement in the electronic conductivity of PEDOT:PSS, achieving values between 10 and 136 S cm^{-1} depending on the substituent of the imidazolium ring and counter-ion of the ionic liquid.[24] Moreover, the addition of ionic liquid to polymers is well known in the field of polyelectrolytes where there is a huge enhancement of the ionic conductivity.[25] However, the few publications with a study of ionic conductivity in conducting polymers[26,27] are based in a range of relative humidity which is not desirable for ESS devices.

Ionic liquids can also be design to be solid, known as organic ionic plastic crystals (OIPCs), by just judicious choice of either the anion or the cation. These OIPCs have attracted much attention for solid-state electrolytes because of their plasticity, low flammability and high ionic conductivity.[28] The compatibility of OIPCs with polymers such as polyvinylidene fluoride (PVdF) or polystyrene (PS) has been seen by Nti. et al.[29] Moreover, our group recently developed for the first time composites of OIPCs with conducting polymers, demonstrating that OIPCs not only can act as electronic and ionic dopants but also improve the mechanical properties of these polymers that are commonly brittle to finally have stable materials with high both ionic and electronic conductivity.[30]

Among the different ways to polymerize EDOT, it is well known that vapor phase polymerization (VPP) leads to high electronic conductivity by creating thin layers with less defects than other techniques.[31] Even though studies relating to depositing larger quantities of PEDOT in 3D structures by VPP have been reported,[32] currently only limited quantity of material is possible and hence, oxidative chemical polymerization is widely used to obtain PEDOT. In this work, PEDOT-Cl was synthesized by oxidative polymerization to mix with the OIPC N-ethyl-N-methylpyrrolidinium bis(fluorosulfonyl)imide ([C_2mpyr][FSI]) at different ratios. This OIPC has been widely studied and applied in Electrochemical Energy Storage systems (EES), as it has a relatively wide plastic crystalline range.[33,34] The composites comprising of PEDOT-Cl and [C_2mpyr][FSI] have been studied in terms of thermal behaviour, morphology, electronic-ionic conductivity and electrochemical performance.

2. EXPERIMENTAL SECTION

2.1. Synthesis of [C_2mpyr][FSI]

The organic ionic plastic crystal N-ethyl-N-methylpyrrolidinium bis(fluoromethanesulfonyl)imide, [C_2mpyr][FSI], was synthesized by a salt metathesis reaction between N-ethyl-N-methylpyrrolidinium bromide, (abcr, [C_2mpyr]Br), with potassium bis(fluoromethanesulfonyl)imide (Fluorochem, KFSI), following the previously reported method.[35]

2.2. Synthesis of PEDOT-Cl

The synthesis of PEDOT-Cl was done by the oxidation polymerization of 3,4-ethylenedioxythiophene (EDOT, Sigma Aldrich), with iron(III) chloride hexahydrate, ($FeCl_3 \cdot 6H_2O$) in acetonitrile, as reported previously.[12]

2.3. Preparation of PEDOT-Cl/[C_2mpyr][FSI] composites

The corresponding amounts of dried PEDOT-Cl and [C_2mpyr][FSI] were carefully mixed with an agate mortar and pestle to obtain composites with PEDOT-Cl/[C_2mpyr][FSI] weight ratios of 10/90, 20/80, 30/70, 40/60 and 50/50. The mixtures were then pressed at 60 ℃ under 4 tons of pressure to obtain the corresponding films. The films were dried under vacuum at 60 ℃ before further characterization.

2.4. Composite characterization

Differential scanning calorimetry (DSC) measurements were carried out on a DSC Q2000 from TA Instruments in order to determine the solid-solid phase transitions and melting temperatures (Tm) of the composites. The samples were first cooled to -80 ºC, then heated to 210 ℃ and cooled again to 25 ℃ at 10 ℃ min^{-1}.

Thermal stability of the composites was investigated with a thermo-gravimetric analysis (TGA) performed on a TGA Q500 from TA Instruments. Measurements were carried out by heating the samples at 10 °C min^{-1} under nitrogen atmosphere from 40 °C to 800 °C.

Fourier Transform Infrared Spectroscopy measurements (FTIR) were conducted on a Nicolet Magna 6700 spectrometer. The samples were mixed with KBr and pressed at room temperature under 10 tons to obtain pellets.

Morphology of the samples was studied by Scanning electron microscope (SEM) analysis using a JEOL JSM-6490LV at 15kV and sputter-coated with gold (Alto 1000, Gatan Inc.). The composite films were cut in circular shapes and stuck onto an aluminum holder with the help of double side carbon tape. The holder was inserted in a vacuum chamber overnight in order to homogenize the pressure. After that, sputter-coated was performed during 60 seconds. Finally, the holder was inserted in the SEM chamber and evaluated in a point by point scanning mode.

The ionic conductivity of the composites was measured by electrochemical impedance spectroscopy using a VMP-3 potentiostat (Biologic Science Instruments). The samples were placed between two stainless steel discs and sealed in a coin cell under argon atmosphere. A frequency range of 1 MHz to 100 mHz was studied using a voltage amplitude of 10 mV. The sample was heated from 25 ℃ to 90 ℃ and measurements were performed every 10 ℃. Then, measurements were repeated cooling the samples from 90 ℃ to 25 ℃. The reported values are the average between the heating and cooling measurements. The samples were equilibrated for 30 minutes before each measurement.

The activation energies (Ea) were extracted from the linear regression of the Arrhenius plots, taking into account the Arrhenius equation:

$$\sigma = \sigma_0 \exp(\frac{-E_a}{k_B T}) \qquad (1)$$

where σ_0 is the dc conductivity of pre-exponential factor, T the absolute temperature, E_a the activation energy and k_B the Boltzmann constant.

The electronic conductivity of the composite films was measured with a FPP 5000 four point probe (Miller Design & Equipment, INC) at room temperature.

2.5. Electrochemical characterization

Cyclic voltammetry was performed in a three-electrode set up, with platinum wire as counter electrode and Ag/AgCl as reference electrode using a VMP-3 potentiostat (Biologic Science Instruments). The composite mixtures were dispersed in methanol (0.1g/mL) and drop-casted (3-5 μL) into a platinum electrode. The obtained electrodes were dried first at room temperature and under vacuum at 60°C for 30 min before the measurement. A 0.1 M KFSI aqueous solution was used as electrolyte, which was purged with nitrogen for 15 min before the experiment. Cyclic voltammetry was carried out in the potential range of -1 V to 1 V vs. Ag/AgCl at different scan rates.

The cycling stability of the optimal composite 40/60 PEDOT-Cl/[C_2mpyr][FSI] was studied in a three-electrode setup by galvanostatic charge-discharge (GCD) at 1 A g^{-1} in a voltage window of 0 - 0.8 V during 1000 cycles. The material was drop casted on carbon paper to finally obtain two electrodes with different mass loadings of composite, 4.8 and 9.4 mg cm^{-2}, named low and high loading electrodes respectively. Both the rate and the gravimetric capacitance were calculated respect to the mass of the redox active component of the composite (PEDOT). The capacitance of the not covered carbon paper was calculated and estimated negligible versus the capacitance given by PEDOT.

3. RESULTS AND DISCUSSION

3.1. Preparation of composite materials

The composites were prepared by solid mixing the corresponding amounts of PEDOT-Cl polymer and [C_2mpyr][FSI] plastic crystal to obtain composites with PEDOT-Cl/[C_2mpyr][FSI] weight ratios of 10/90, 20/80, 30/70, 40/60 and 50/50 (Figure 1). The mixtures were then pressed at 60 °C under 4 tons of pressure to obtain the corresponding films.

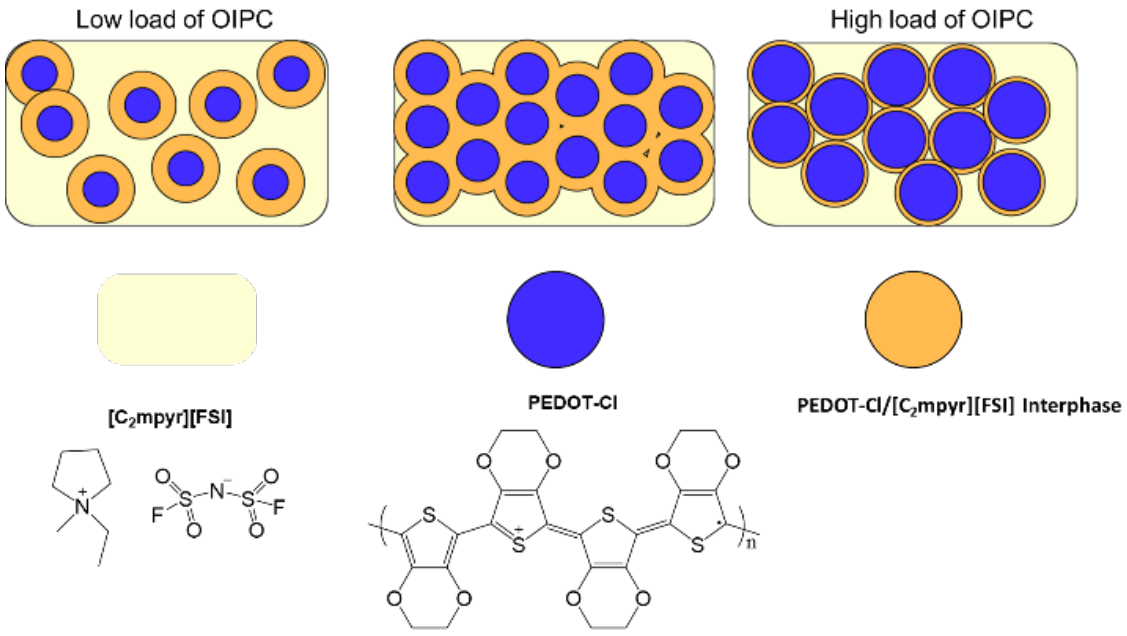

Figure 1. Schematic representation of composite films with PEDOT:Cl-rich (blue) and [C_2mpyr][FSI]-rich (yellow) phases and their chemical structure.

3.2. Characterization of the composites

Differential scanning calorimetry (DSC) measurements were performed to analyse the thermal properties of the composites with different amounts of PEDOT polymer and plastic crystal. As can be observed in Figure 2, the neat [C_2mpyr][FSI] plastic crystal presents two solid-solid phase

transitions at -67 ℃ and -22 ℃ and a melting behaviour at 202 ℃, as previously reported.[36] The highest temperature phase is named phase I, while the following lower temperature phases are phase II and III.[36]

PEDOT-Cl/[C_2mpyr][FSI] composites present the three transitions, except for the 50/50 composite where the solid-solid transitions have disappeared, indicating a disordered behaviour. It can be observed that the incorporation of PEDOT to the OIPC matrix results in the clear decrease of the melting temperature from 202 ℃ (for pure OIPC) to 61℃ (for 40/60 composite), together with the entropy decrease of solid-solid transitions. Similar changes has been observed by other authors in PVdF/OIPC[29,37] and PVdF/IL[38] composites suggesting the existence of certain interaction between polymer and salt. When PEDOT is introduced in the OIPC matrix, an interphase is created between the PEDOT particles and the plastic crystal, which induces disorder in the OIPC matrix, thereby decreasing the entropy value of solid-solid transitions. This disorder results from motions (such as side-chain movements, rotation or translation) of the OIPC cations or anions, which lead to the plastic behaviour.[39] At 50/50 composition, the interphases created are higher and the OIPC is not able to create ordered domains, resulting in an amorphous material and thus, no solid-solid state transition is observed in the DSC curve.

Figure S1 shows the TGA curves of [C_2mpyr][FSI] and the composites. The degradation of neat OIPC occurs around 330 ℃ in one single step, while the composites show various degradation steps. At low PEDOT content (10/90 composite) a small initial degradation is observed at 290 ℃ related to the PEDOT chains and a second main degradation at 365 ℃ corresponding to the OIPC. At intermediate compositions (20/80, 30/70, 40/60 composites) a new degradation step is observed at 230 ℃ together with the 209 ℃ and 360 ℃ steps. This new step at lower temperatures can be related to the interphase domains between the OIPC and PEDOT. Finally, at high PEDOT content

(50/50 composite) two degradation steps are observed, the main one at 310 ℃ and the second as a shoulder at 360 ℃, related to the PEDOT and OIPC degradations. All the composites present high thermal stability, 270, 257, 227, 223, 250 ℃ where 5 wt.% of the mass is being lost.

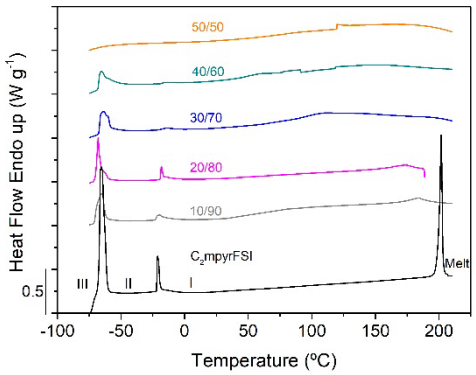

Figure 2. DSC heating traces (first heating scan) of neat [C_2mpyr][FSI] (black) and different PEDOT-Cl/[C_2mpyr][FSI] composites as shown in the figure legends.

Infrared spectroscopy was employed to perform the structural characterization of the composites. Figure S2 shows the FTIR spectra of 50/50 composite and the pure components PEDOT-Cl and [C_2mpyr][FSI]. The neat [C_2mpyr][FSI] presents peaks at 1465, 1096, 1031, 997, 936 cm^{-1} corresponding to the C_2mpyr cation, while the peaks at 1376, 1359, 1216, 1165, 822 and 719 cm^{-1} are attributed to the FSI anion.[40] It can be observed that the main peaks of the composite are related to the plastic crystal. Major differences can be observed in the peaks attributed to the FSI anion (1376, 1165, 719 cm^{-1}) which are shifted to higher wavenumbers in the composite and also the peak at 1376 cm^{-1} has increased its intensity. These changes in the FSI vibration bands suggest the presence of ion interactions between charged PEDOT and the FSI anions in the plastic crystal.[41]

The morphology of the composites was studied by Scanning Electron Microscopy (SEM). In order to compare, we selected the composites with the composition of 20/80 and 40/60. As can be observed in Figure 3 and Figure S3, the film of 20/80 composite presents a heterogeneous surface, while 40/60 composite is a homogeneous film. We can observe in 20/80 composite that PEDOT particles are distributed unevenly in the OIPC matrix, therefore, some parts are richer in OIPC, while others are agglomerates of PEDOT. In contrast, 40/60 sample, presents a homogeneous surface, where PEDOT particles are surrounded by the plastic crystal.

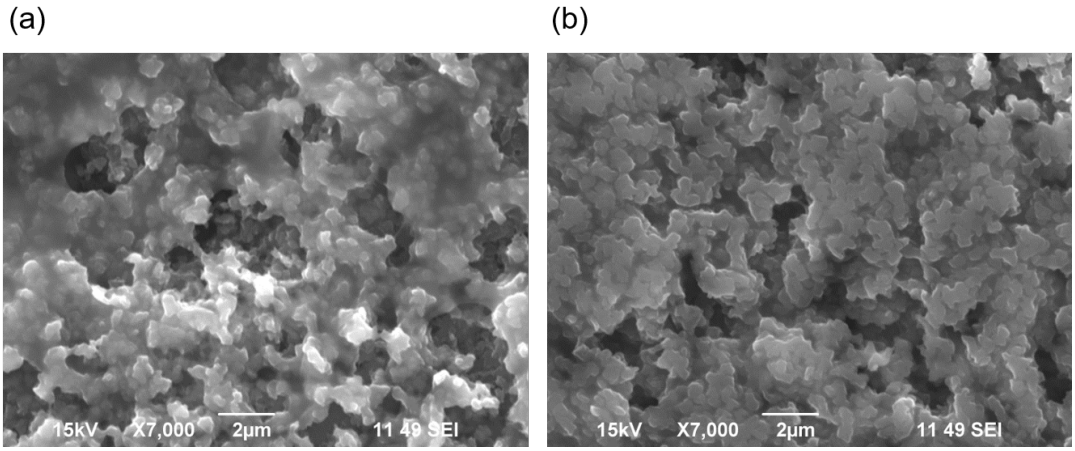

Figure 3. SEM images of (a) 20/80 and (b) 40/60 PEDOT-Cl/[C_2mpyr][FSI] composites.

3.3. Ionic and electronic conductivities of the composites

The transport properties of the composites were analysed measuring the ionic conductivity by electrochemical impedance spectroscopy (EIS) and the electronic conductivity by four-point-probe method. During the EIS measurements the typical closed semicircle for MIECs was observed and the electronic resistance was taken as negligible versus the ionic resistance as others authors have suggested.[42] Figure 4a shows the ionic conductivities of neat [C_2mpyr][FSI] and

PEDOT-Cl/[C_2mpyr][FSI] composites at various temperatures. It can be observed that the ionic conductivity increases with the increment of PEDOT content in the composite, obtaining the best conductivity values for 40/60 and 50/50 composites, $2.3 \cdot 10^{-4}$ and $3.0 \cdot 10^{-4}$ S cm^{-1} at 25 °C, respectively. This is in good agreement with the DSC results, where the increase of PEDOT content resulted in a decrease of crystalline phases and thus, higher ionic conductivity. However, the 10/90 composite doesn't follow this trend and its ionic conductivity is below the neat [C_2mpyr][FSI]. This behaviour is not currently understood, however, here we focus on the higher OIPC containing MIECs. It can be also observed that with higher PEDOT content, the conductivity is less dependent on temperature, thus, having a low activation energy (1.65 kJ mol^{-1} for 40/60 composite, Figure 4b and Figure S4). Figure 4b shows the ionic and electronic conductivities at room temperature at different PEDOT-Cl concentrations in the composites. As expected, the electronic conductivity increases with PEDOT content, as there are more electronically conductive PEDOT particles in the composite. At low concentrations these particles are likely sparsely distributed and well separated from each other (i.e. they do not touch), as was observed in the SEM images of 20/80 composite (Figure 3a). However, when the concentration increases the PEDOT particles start to be connected, having longer electronic pathways and thus, higher electronic conductivity. It is worth mentioning that the electronic conductivity of neat PEDOT-Cl was 2.1 S cm^{-1}, which is in the range of values of PEDOT-Cl synthesized by oxidative polymerization,[43,44] while the optimum value (17.7 S cm^{-1}) is obtained at 40/60 concentration with a slow decrease in 50/50 composite (14.6 S cm^{-1}). This decrease could be related to the amorphous behaviour of the composite observed in the DSC, as it has been proven that crystalline domains in PEDOT provide higher electrical conductivity.[45,46] Thus, the crystalline phases of the plastic crystal might induce alignment of PEDOT films, improving the electronic conductivity of neat PEDOT-Cl. It can be

also observed that the ionic conductivity at room temperature increases with PEDOT content, due to the disorder created by PEDOT particles in the plastic crystal, and stabilizing after 40/60 composition. Therefore, we can conclude that the highest ionic and electronic conductivities were obtained with 40/60 composite, where the crystal nature of the OIPC is still preserved.

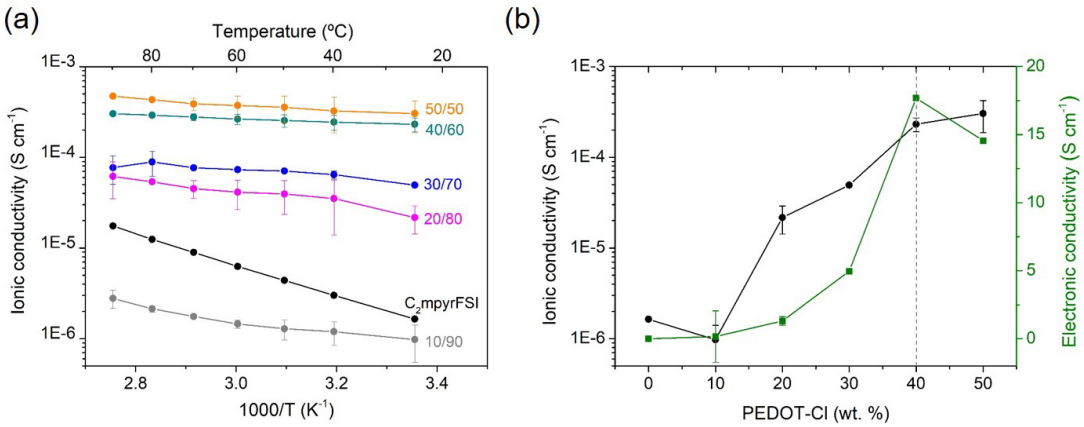

Figure 4. (a) Ionic conductivity as function of temperature of neat [C_2mpyr][FSI] (black) and different PEDOT-Cl/[C_2mpyr][FSI] composites as shown in the figure legends, (b) Ionic (black) and electronic (green) conductivities at 25 ºC as function of PEDOT-Cl concentration in the composites.

3.4. Electrochemical properties of the composites

The electrochemical properties of the composites were evaluated by cyclic voltammetry (CV) using a three-electrode cell in 0.1 M KFSI aqueous electrolyte to establish the activity of the PEDOT in this composite. Aqueous electrolyte was chosen to study the electrochemistry because [C_2mpyr][FSI] is not soluble in water and thus, the integrity of the electrode was preserved. The working electrode was coated with the composite films, without the need of additional binder. Figure 5a shows the CV curves of 40/60 PEDOT-Cl/[C_2mpyr][FSI] composite at different scan

rates. We can observe broad anodic and cathodic peaks which are typical of PEDOT materials.[47] Figure S5 shows that anodic and cathodic currents are proportional to the scan rate, indicating that the redox process is not limited by diffusion, demonstrating that the entire film is involved in the redox reaction.[48] Comparing the cyclic voltammograms of the different composites and neat PEDOT (Figure 5b), it can be observed that the current density increases with the amount of PEDOT in the composite, as expected, due to its electroactivity. However, we can observe that the maximum oxidation current is obtained with the 40/60 composite, being very similar to neat PEDOT, which can be attributed also to the higher electronic conductivity of this composite, as shown before.

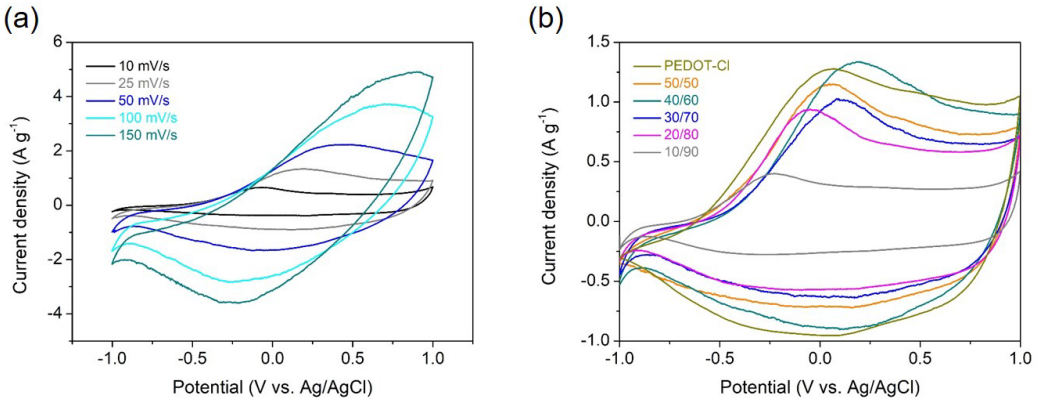

Figure 5. (a) Cyclic voltammetry of PEDOT-Cl/[C2mpyr][FSI] 40/60 composite at different scan rates, as shown in the figure legends. (b) Comparison of cyclic voltammetries of neat PEDOT-Cl and different PEDOT-Cl/[C2mpyr][FSI] composites, as shown in the figure legends, at a scan rate of 25 mV s^{-1} and 0.1 M KFSI aqueous electrolyte.

The cycling stability of the optimal composite 40/60 PEDOT-Cl/[C2mpyr][FSI] was studied by galvanostatic charge-discharge at 1 A g^{-1}. The highest gravimetric capacitance was obtained with the low loading electrode as expected, which showed 103 F g^{-1} capacitance in the 5th cycle and a

retention of 79 % after 1000 cycles, as can be observed in Fig. S7. This capacitance value is higher than previously reported PEDOT-Cl work[12] which showed 92.8 F g^{-1} in a three electrode setup with significantly lower mass loading, as can be seen in Table 1.

Table 1. Specific capacitances and experiment conditions of this system compared with other similar PEDOT works.

Electrode		Mass Loading (mg cm^{-2})	Test Condition	Gravimetric Capacitance (F g^{-1})	Areal Capacitance (mF cm^{-2})
This work PEDOT-OIPC / Carbon paper	0.1 M KFSI	4.8	1 A g^{-1} 1.92 mA cm^{-2}	103	198
		9.4	1 A g^{-1} 3.76 mA cm^{-2}	79	296
PEDOT / Carbon paper[12]	emim dca	1.8	1 A g^{-1} 1.8 mA cm^{-2}	92.8	170
PEDOT / Carbon paper[49]	$BMIBF_4$/ PVdF-HFP	1	1 A g^{-1} 1 mA cm^{-2}	154.5	85
PEDOT / Cellulose paper[50]	PVA – H_2SO_4	1	0.4 A g^{-1} 0.4 cm^{-2}	115	115

Emim dca: 1-ethyl-3-methylimidazolium dicyanamide, $BMIBF_4$: 1-butyl-3-methylimidazolium tetrafluoroborate, PVDF-HFP: poly(vinylidene fluoride hexafluoropropylene).

Overall, low loading electrodes are more likely to provide higher specific capacitances per mass, as ions and electrons can be easily transferred in really thin electrodes. However, high mass loading electrodes are necessary for practical applications to increase the energy density of the system, becoming the areal capacitance a key parameter to consider. For this reason, we tested a high loading 40/60 PEDOT-Cl/[C_2mpyr][FSI] electrode, which showed an areal capacitance of 296 mF cm^{-2} in the 5th cycle and a capacitance retention of 87 % after 1000 cycles, with coulombic efficiencies close to 100 %, as can be observed in Fig. 6. Despite showing an iR drop of 150 mV, 40/60 PEDOT-Cl/[C_2mpyr][FSI] electrode showed stable cycling stability, with a sloppy voltage

profile typical for PEDOT based materials, which maintains almost the same after 1000 cycles. The high areal capacitance obtained demonstrates the effective coupling of ionic-electronic transport in the composite, which is essential to achieve high energy density materials.

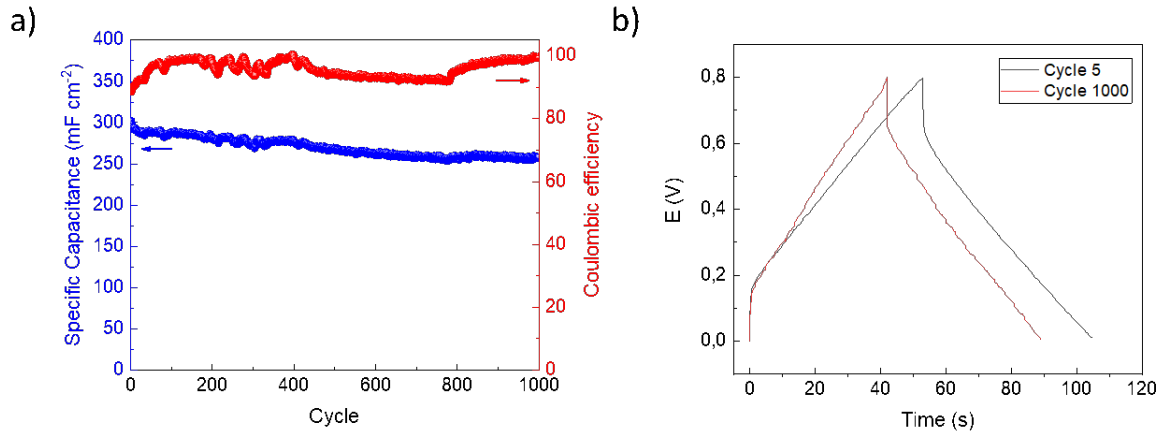

Figure 6. a) Specific capacitance, coulombic efficiency and b) charge-discharge profiles of the high loading 40/60 PEDOT-Cl/[C_2mpyr][FSI] electrode at 1 A g^{-1}. The temperature of the system was kept constant at 30 °C.

4. CONCLUSION

In this work, synthesis and characterization of a mixed ionic and electronic conducting material with redox activity was carried out by mixing a conducting polymer (PEDOT-Cl) and the OIPC [C_2mpyr][FSI]. The conducting polymer PEDOT-Cl was synthesized by oxidative polymerization obtaining an electronic conductivity of 2.1 S cm^{-1}, which is in the range of pristine PEDOT:PSS (0.1-1 S cm^{-1})[51] and an ionic conductivity of around $2 \cdot 10^{-6}$ S cm^{-1} at room temperature.

The addition of OIPC to a conducting polymer has been studied providing promising results with an enhancement of ×9 for electronic conductivity (17.7 S cm^{-1}) and ×180 for ionic in the 40/60

PEDOT-Cl/[C_2mpyr][FSI] composite. Surprisingly, ionic conductivity values of around 10^{-4} S cm^{-1} at room temperature were obtained, which might be due to the formation of highly conducting pathways through the interphase of PEDOT-Cl and [C_2mpyr][FSI] as has been suggested for OIPC/PVdF composites.[29,37] It is important to note that, these ionic conductivity values are really close to the desirable range of solid electrolytes (~10^{-3} S cm^{-1}) in the field of energy storage systems.[52] Furthermore, the activation energy for conduction in these composites was very low as observed in the Arrhenius representation of ionic conductivity versus inverse temperature (Figure S3). This is an interesting observation that needs further investigation to understand the change in conduction mechanism in these composites compared to the pure OIPCs.

Redox activity was observed in all the composites, even showing an improvement in the case of 40/60 PEDOT-Cl/[C_2mpyr][FSI] with respect to the neat PEDOT-Cl; likely due to the increased electronic conductivity. High mass loading 40/60 PEDOT-Cl/[C_2mpyr][FSI] electrodes showed high capacitance values of 296 mF cm^{-2} and retained 87 % of capacitance after 1000 cycles. Hence we demonstrate that the OIPC [C_2mpyr][FSI] has an interesting synergistic effect in the composite material with PEDOT-Cl, not only in the electronic and ionic conductivity but also in the redox activity and capacitance values. This opens up the possibility of designing MIEC from composites based on conducting polymers and OIPCs as ideal candidates for future electrochemical devices. There is much scope for designing these materials with different redox polymers and counterions other than Cl^- as well as different OIPCs targeted to specific applications.

ASSOCIATED CONTENT

Supporting Information. Table S1: Phase transition onset temperatures and entropies of pure [C_2mpyr][FSI] and composites with PEDOT-Cl. Figures S1-S7: Thermogravimetric analysis of neat [C_2mpyr][FSI] and different PEDOT-Cl/[C_2mpyr][FSI] composites; FT-IR spectra of neat PEDOT-Cl, [C_2mpyr][FSI] and 50/50 PEDOT-Cl/[C_2mpyr][FSI] composite; SEM images of 20/80 and 40/60 PEDOT-Cl/[C_2mpyr][FSI] composites; Arrhenius plot and activation energies calculated from Arrhenius plots for pure [C_2mpyr][FSI] and composites with PEDOT-Cl; anodic and cathodic peak current dependence over the scan rate of 40/60 PEDOT-Cl/[C_2mpyr][FSI] composite; cyclic voltammetries in 0.1 M KFSI aqueous electrolyte of PEDOT-Cl/[C_2mpyrFSI] composites and neat PEDOT-Cl; specific capacitance and coulombic efficiency of the low loading 40/60 PEDOT-Cl/**[**C_2mpyr**][**FSI**]** electrode.

AUTHOR INFORMATION

Corresponding Author

*N. Casado. E-mail: Nerea.casado@ehu.eus

*M. Forsyth. E-mail: maria.forsyth@deakin.edu.au

Funding Sources

This work was supported by an Ikerbasque Research Fellowship from the Basque Government and the European Commission through funding from the European Union's Horizon 2020 research and innovation program under the Marie Sklodowska-Curie grant agreement No 823989.

Notes

There are no conflicts to declare.

ACKNOWLEDGMENT

This work was supported by an Ikerbasque Research Fellowship from the Basque Government and the European Union's Horizon 2020 research and innovation program under the Marie Sklodowska-Curie grant agreement No 823989. NC would like to thank the University of the Basque Country for funding through a specialization of research staff fellowship (ESPDOC 19/99).

ABBREVIATIONS

MEA, membrane electrode assemblies; PVdF, polyvinylidene fluoride; MIECs, mixed ionic-electronic conductors; PEDOT:PSS, poly(3,4-ethylenedioxythiphene):polystyrene; OIPC, organic ionic plastic crystal; VPP, vapor phase polymerization; EDOT, 3,4-ethylenedioxythiophene; [C_2mpyr][FSI], N-ethyl-N-methylpyrrolidinium bis(fluorosulfonyl)imide; PEDOT-Cl, poly(3,4-ethylenedioxythiphene) chloride.

REFERENCES

(1) Paulsen, B. D.; Tybrandt, K.; Stavrinidou, E.; Rivnay, J. Organic Mixed Ionic – Electronic Conductors. *Nat. Mater.* **2020**, *19*, 13–26.

(2) Aurbach, D. Review of Selected Electrode–Solution Interactions Which Determine the Performance of Li and Li Ion Batteries. *J. Power Sources* **2000**, *89*, 206–218.

(3) Sunarso, J.; Baumann, S.; Serra, J. M.; Meulenberg, W. A.; Liu, S.; Lin, Y. S.; Diniz, J. C. Mixed Ionic-Electronic Conducting (MIEC) Ceramic-Based Membranes for Oxygen Separation. *J. Memb. Sci.* **2008**, *320*, 13–41.

(4) Chueh, W. C.; Haile, S. M. Electrochemistry of Mixed Oxygen Ion and Electron Conducting Electrodes in Solid Electrolyte Cells. *Annu. Rev. Chem. Biomol. Eng.* **2012**, *3*, 313–341.

(5) Malti, A.; Edberg, J.; Granberg, H.; Khan, Z. U.; Andreasen, J. W.; Liu, X.; Zhao, D.;

Zhang, H.; Yao, Y.; Brill, J. W.; Engquist, I. An Organic Mixed Ion – Electron Conductor for Power Electronics. *Adv. Sci.* **2016**, *3*, 1–9.

(6) Wu, M.; Xiao, X.; Vukmirovic, N.; Xun, S.; Das, P. K.; Song, X.; Olalde-velasco, P.; Wang, D.; Weber, A. Z.; Wang, L.; Battaglia, V. S.; Yang, W.; Liu, G. Toward an Ideal Polymer Binder Design for High-Capacity Battery Anodes. *J. Am. Chem. Soc.* **2013**, *135*, 12048–12056.

(7) Bobacka, J. Conducting Polymer-Based Solid-State Ion-Selective Electrodes. *Electroanalysis* **2006**, No. 1, 7–18.

(8) Nilsson, D.; Robinson, N. D.; Isaksson, J.; All, P. K. J.; Berggren, M.; Richter-dahlfors, A. Electronic Control of Ca2 + Signalling in Neuronal Cells Using an Organic Electronic Ion Pump. *Nat. Mater.* **2007**, *6*, 673–679.

(9) Alam, M. M.; Wang, J.; Guo, Y.; Lee, S. P.; Tseng, H. Electrolyte-Gated Transistors Based on Conducting Polymer Nanowire Junction Arrays. *J. Phys. Chem. B* **2005**, *109*, 12777–12784.

(10) Yigitsoy, B.; Varis, S.; Tanyeli, C.; Akhmedov, I. M.; Toppare, L. A Soluble Conducting Polymer of 2 ,5-Di(Thiophen-2-Yl)-1-p-Tolyl-1H-Pyrrole and Its Electrochromic Device. *Thin Solid Films* **2007**, *515*, 3898–3904.

(11) Shi, Y.; Peng, L.; Yu, G. Nanostructured Conducting Polymer Hydrogels for Energy Storage Applications. *Nanoscale* **2015**, *7*, 12796–12806.

(12) Karlsson, C.; Nicholas, J.; Evans, D.; Forsyth, M.; Sjçdin, M.; Howlett, P. C.; Pozo-

Gonzalo, C. Stable Deep Doping of Vapor-Phase Polymerized Poly (3,4-Ethylenedioxythiophene)/ Ionic Liquid Supercapacitors. *ChemSusChem* **2016**, *9*, 2112–2121.

(13) Xia, Y.; Ouyang, J. Significant Different Conductivities of the Two Grades of Poly(3,4-Ethylenedioxythiophene):Poly(Styrenesulfonate), Clevios P and Clevios PH1000, Arising from Different Molecular Weights. *Appl. Mater. Interfaces* **2012**, *4*, 4131–4140.

(14) You, A.; Be, M. A. Y.; In, I. Doping Level and Work Function Control in Oxidative Chemical Vapor Deposited Poly (3,4-Ethylenedioxythiophene). *Appl. Phys. Lett.* **2007**, *90*, 152112.

(15) Okuzaki, H.; Harashina, Y.; Yan, H. Highly Conductive PEDOT/PSS Microfibers Fabricated by Wet-Spinning and Dip-Treatment in Ethylene Glycol. *Eur. Polym. J.* **2009**, *45*, 256–261.

(16) Ouyang, J. '"Secondary Doping"' Methods to Significantly Enhance the Conductivity of PEDOT : PSS for Its Application as Transparent Electrode of Optoelectronic Devices. *Displays* **2013**, *34*, 423–436.

(17) Luo, J.; Billep, D.; Waechtler, T.; Otto, T.; Toader, M.; Gordan, O.; Sheremet, E.; Martin, J.; Hietschold, M.; Zahn, D. R. T.; Gessner, T. Enhancement of the Thermoelectric Properties of PEDOT:PSS Thin Films by Post-Treatment. *J. Mater. Chem. A* **2013**, *1*, 7576.

(18) Sato, K.; Dutta, M.; Fukata, N. Inorganic/Organic Hybrid Solar Cells: Optimal Carrier Transport in Vertically Aligned Silicon Nanowire. *Nanoscale* **2014**, 6092–6101.

(19) Khan, Z. U.; Bubnova, O.; Jafari, J.; Brooke, R.; Liu, X.; Gabrielsson, R.; Ederth, T.; Evans, D. R.; Andreasen, J. W.; Crispin, X. Acido-Basic Control of the Thermoelectric Properties of Poly(3,4-Ethylenedioxythiophene)Tosylate (PEDOT-Tos) Thin Films. *J. Mater. Chem. C* **2015**, *3*, 10616–10623.

(20) Pistillo, B. R.; Menguelti, K.; Desbenoit, N.; Arl, D.; Leturcq, R.; Ishchenko, O. M.; Kunat, M.; Baumann, P. K.; Lenoble, D. One Step Deposition of PEDOT Films by Plasma Radicals Assisted Polymerization via Chemical Vapour Deposition †. *J. Mater. Chem. C* **2016**, *4*, 5617–5625.

(21) Meng, W.; Ge, R.; Li, Z.; Tong, J.; Liu, T.; Zhao, Q.; Xiong, S.; Jiang, F.; Mao, L.; Zhou, Y. Conductivity Enhancement of PEDOT:PSS Films via Phosphoric Acid Treatment for Flexible All-Plastic Solar Cells. *Appl. Mater. Interfaces* **2015**, *7*, 14089–14094.

(22) Kee, S.; Kim, N.; Kim, B. S.; Park, S.; Jang, Y. H.; Lee, S. H.; Kim, J.; Kim, J.; Kwon, S.; Lee, K. Controlling Molecular Ordering in Aqueous Conducting Polymers Using Ionic Liquids. *Adv. Mater.* **2016**, *28*, 8625–8631.

(23) John, C.; Higgins, T. M.; Park, S.; Brien, S. E. O.; Long, D.; Coleman, J. N.; Nicolosi, V. Highly Flexible and Transparent Solid-State Supercapacitors Based on RuO2/PEDOT:PSS Conductive Ultra Thin Films. *Nano Energy* **2016**, *28*, 495–505.

(24) Döbbelin, M.; Marcilla, R.; Salsamendi, M.; Pozo-gonzalo, C.; Carrasco, P. M.; Pomposo, J. A.; Mecerreyes, D. Influence of Ionic Liquids on the Electrical Conductivity and Morphology of PEDOT:PSS Films. *Chem. Mater.* **2007**, *19* (9), 2147–2149.

(25) Demarteau, J.; Fdz. de Añastro, A.; Shaplov, A. S. Poly(Diallyldimethylammonium) Based

Poly(Ionic Liquid) Di- and Triblock Copolymers by PISA as Matrices for Ionogel Membranes. *Polym* **2020**, *11*, 1481–1488.

(26) Malti, A.; Edberg, J.; Granberg, H.; Khan, Z. U.; Andreasen, J. W.; Liu, X.; Zhao, D.; Zhang, H.; Yao, Y.; Brill, J. W.; Engquist, I. An Organic Mixed Ion–Electron Conductor for Power Electronics. *Adv. Sci.* **2016**, *3*, 150035.

(27) Wang, H.; Ail, U.; Gabrielsson, R.; Berggren, M.; Crispin, X. Ionic Seebeck Effect in Conducting Polymers. *Adv. Energy Mater.* **2015**, *5*, 1500044.

(28) Basile, A.; Hilder, M.; Makhlooghiazad, F.; Pozo-gonzalo, C.; Macfarlane, D. R.; Howlett, P. C.; Forsyth, M. Ionic Liquids and Organic Ionic Plastic Crystals : Advanced Electrolytes for Safer High Performance Sodium Energy Storage Technologies. *Adv. Funct. Mater.* **2018**, *1703491*, 1–20.

(29) Nti, F.; Porcarelli, L.; Greene, G. W.; Zhu, H.; Makhlooghiazad, F.; Mecerreyes, D.; Howlett, P. C.; Forsyth, M.; Wang, X. The Influence of Interfacial Interactions on the Conductivity and Phase Behaviour of Organic Ionic Plastic Crystal/Polymer Nanoparticle Composite Electrolytes. *J. Mater. Chem. A* **2020**, *8*, 5350–5362.

(30) Del Olmo, R.; Casado, N.; Olmedo-Martinez, J. L.; Wang, X.; Forsyth, M. Mixed Ionic-Electronic Conductors Based on PEDOT : PolyDADMA and Organic Ionic Plastic Crystals. *Polymers (Basel).* **2020**, *12*, 1981.

(31) Li, J.; Zhang, M.; Liu, J.; Ma, Y. Effect of Attached Peroxyacid on Liquid Phase Depositional Polymerization of EDOT over PI Film with Adsorbed Ferric Chloride. *Synth. Met.* **2014**, *198*, 161–166.

(32) Dominguez-Alfaro, A.; Alegret, N.; Arnaiz, B.; González-Domínguez, J. M.; Martin-Pacheco, A.; Cossío, U.; Porcarelli, L.; Bosi, S.; Vázquez, E.; Mecerreyes, D.; Prato, M. Tailored Methodology Based on Vapor Phase Polymerization to Manufacture PEDOT/CNT Scaffolds for Tissue Engineering. *ACS Biomater. Sci. Eng.* **2020**, *6* (2), 1269–1278.

(33) Best, A. S.; Bhatt, A. I.; Hollenkamp, A. F. Ionic Liquids with the Bis(Fluorosulfonyl)Imide Anion: Electrochemical Properties and Applications in Battery Technology. *J. Electrochem. Soc.* **2010**, *157* (8), A903.

(34) Zhou, Y.; Wang, X.; Zhu, H.; Armand, M.; Forsyth, M.; Greene, G. W.; Pringle, M.; Howlett, P. C. N-Ethyl-N-Methylpyrrolidinium Bis(Fluorosulfonyl)Imide-Electrospun Polyvinylidene Fluoride Composite Electrolytes: Characterization and Lithium Cell Studies †. *Phys. Chem. Chem. Phys.* **2017**, *19*, 2225–2234.

(35) Yunis, R.; Newbegin, T. W.; Hollenkamp, A. F.; Pringle, J. M. Ionic Liquids and Plastic Crystals with a Symmetrical Pyrrolidinium Cation †. *Mater. Chem. Front.* **2018**, *2*, 1207–1214.

(36) Yoshizawa-Fujita, M.; Kishi, E.; Suematsu, M.; Takekawa, T.; Rikukawa, M. A Plastic Electrolyte Material in a Highly Desirable Temperature Range: *N* -Ethyl- *N* -Methylpyrrolidinium Bis(Fluorosulfonyl)Amide. *Chem. Lett.* **2014**, *43* (12), 1909–1911.

(37) Wang, X.; Zhu, H.; Greene, G. W.; Li, J.; Iranipour, N.; Garnier, C.; Fang, J.; Armand, M.; Forsyth, M.; Pringle, J. M.; Howlett, P. C. Enhancement of Ion Dynamics in Organic Ionic Plastic Crystal/PVDF Composite Electrolytes Prepared by Co-Electrospinning. *J. Mater. Chem. A* **2016**, *4* (25), 9873–9880.

(38) Mejri, R.; Dias, J. C.; Lopes, A. C.; Hentati, S. B.; Silva, M. M.; Botelho, G.; Ferro, A. M. De; Esperança, J. M. S. S.; Maceiras, A.; Laza, J. M.; Vilas, J. L.; León, L. M.; Lanceros-mendez, S. Effect of Ionic Liquid Anion and Cation on the Physico-Chemical Properties of Poly (Vinylidene Fluoride)/Ionic Liquid Blends. *Eur. Polym. J.* **2015**, *71*, 304–313.

(39) Zhou, Y.; Wang, X.; Zhu, H.; Armand, M.; Forsyth, M.; Greene, G. W.; Pringle, J. M.; Howlett, P. C. N-Ethyl-N-Methylpyrrolidinium Bis(Fluorosulfonyl)Imide-Electrospun Polyvinylidene Fluoride Composite Electrolytes: Characterization and Lithium Cell Studies. *Phys. Chem. Chem. Phys.* **2017**, *19* (3), 2225–2234.

(40) Li, X.; Zhang, Z.; Li, S.; Yang, K.; Yang, L. Polymeric Ionic Liquid-Ionic Plastic Crystal All-Solid-State Electrolytes for Wide Operating Temperature Range Lithium Metal Batteries. *J. Mater. Chem. A* **2017**, *5*, 21362–21369.

(41) Huang, J.; Hollenkamp, A. F. Thermal Behavior of Ionic Liquids Containing the FSI Anion and the Li+ Cation. *J. Phys. Chem. C* **2010**, *114*, 21840–21847.

(42) Mcdonald, M. B.; Hammond, P. T. Efficient Transport Networks in a Dual Electron/Lithium-Conducting Polymeric Composite for Electrochemical Applications. *ACS Appl. Mater. Interfaces* **2018**, *10*, 15681–15690.

(43) Liu, Z.; Zhang, X.; Poyraz, S.; Surwade, S. P.; Manohar, S. K. Oxidative Template for Conducting Polymer Nanoclips. *J. Am. Chem. Soc.* **2010**, *132*, 13158–13159.

(44) Shimogama, N.; Uda, M.; Oyama, K.; Hanochi, H.; Hirai, T. Hydrophobic Poly(3,4-Ethylenedioxythiophene) Particles Synthesized by Aqueous Oxidative Coupling Polymerization and Their Use as near-Infrared-Responsive Liquid Marble Stabilizer.

Polym. J. **2019**, *51*, 761–770.

(45) Wang, X.; Zhang, X.; Sun, L.; Lee, D.; Lee, S.; Wang, M.; Zhao, J.; Shao-horn, Y.; Dinc, M.; Palacios, T.; Gleason, K. K. High Electrical Conductivity and Carrier Mobility in OCVD PEDOT Thin Films by Engineered Crystallization and Acid Treatment. *Sci. Adv.* **2018**, *4*, 5780.

(46) Sirringhaus, H.; Brown, P. J.; Friend, R. H.; Nielsen, M. M.; Bechgaard, K.; Spiering, A. J. H. Two-Dimensional Charge Transport in Self-Organized, High-Mobilityconjugated Polymers. *Nature* **1999**, *401*, 685–688.

(47) Marzocchi, M.; Gualandi, I.; Calienni, M.; Zironi, I.; Scavetta, E.; Castellani, G.; Fraboni, B. Physical and Electrochemical Properties of PEDOT:PSS as a Tool for Controlling Cell Growth. *Appl. Mater. Interfaces* **2015**, *7*, 17993–18003.

(48) Rountree, K. J.; Mccarthy, B. D.; Rountree, E. S.; Eisenhart, T. T.; Dempsey, J. L. A Practical Beginner ’s Guide to Cyclic Voltammetry. *J. Chem. Educ.* **2018**, *95*, 197–206.

(49) Pandey, G. P.; Rastogi, A. C.; Westgate, C. R. All-Solid-State Supercapacitors with Poly(3,4-Ethylenedioxythiophene)- Coated Carbon Fiber Paper Electrodes and Ionic Liquid Gel Polymer Electrolyte. *J. Power Sources* **2014**, *245*, 857–865.

(50) Anothumakkool, B.; Soni, R.; Bhange, S. N.; Kurungot, S. Novel Scalable Synthesis of Highly Conducting and Robust PEDOT Paper for a High Performance Fl Exible Solid Supercapacitor †. *Energy Environ. Sci.* **2015**, 1339–1347.

(51) Shi, H.; Liu, C.; Jiang, Q.; Xu, J. Effective Approaches to Improve the Electrical

Conductivity of PEDOT:PSS: A Review. *Adv. Electron. Mater.* **2015**, *1* (4), 1–16.

(52) Bocharova, V.; Sokolov, A. P. Perspectives for Polymer Electrolytes: A View from Fundamentals of Ionic Conductivity. *Macromolecules* **2020**, *53* (11), 4141–4157.